Energy and Buildings, http://dx.doi.org/10.1016/j.enbuild.2015.05.047

Simple models for building-integrated solar thermal systems

Christoph Maurer*[1], Christoph Cappel[1], Tilmann E. Kuhn[1]

[1]Fraunhofer Institute for Solar Energy Systems ISE, Heidenhofstr. 2, D-79110 Freiburg, Germany

christoph.maurer@ise.fraunhofer.de, christoph.cappel@ise.fraunhofer.de, tilmann.kuhn@ise.fraunhofer.de

*corresponding author: Dr. Christoph Maurer, Fraunhofer ISE, Heidenhofstr. 2, D-79110 Freiburg, Germany, phone +49 761 4588 5667, mobile +49 172 1613886, email christoph.maurer@ise.fraunhofer.de

1. Abstract

Building-integrated solar thermal systems (BIST) outperform building-added solar thermal systems (BAST) due to smaller heat losses at the back of the collector. BIST offer economic advantages, too. The insulation behind the collector can be used to reduce the heating demand of the building as well as to increase the solar thermal yield. Therefore, less material and labour are needed. Of course, the energy flux to the building interior needs to be considered. This energy flux depends in general on the operation of the collector as well as on the irradiance. Several innovative solar thermal building skins have been modelled in detail to analyse this coupling between the active building skin and the building. However, planners need an easy approach to include BIST into their calculations. Often, there is not enough budget to measure and model the new façade. This paper presents several new and simple models which are more accurate than neglecting the coupling to the building and which are less complex than detailed physical models.

Keywords: Building-integrated solar thermal systems (BIST); building-integrated solar systems (BISS); solar architecture; multifunctional façades; building simulation; variable g value; solar thermal façades; nearly-zero energy buildings (NZEB)

2. Introduction

Figure 1 presents a schematic drawing of a building-added and a building-integrated solar thermal collector. Numerous models of solar thermal collectors have been presented. Some of these models are suitable for building-integrated collectors [1-6]. A general overview of BIST modelling and simulation is provided by [7, 8]. With such a detailed model, BIST collectors can be well characterized [9]. However, detailed models need more calculation time than simple models and require some effort to be adjusted to a new collector. The simplest approach is to neglect the building integration and to simulate the collector with an efficiency curve [10] as if it were building-attached and rear-ventilated. This could be called the BAST approach and leads to errors in the calculation of the collector gain and of the energy flux into the building. Analysis of past attempts to find a simple model for a complex BIST façade has shown that the errors at certain time steps can be large and that it is difficult to calculate the heat flux to the building interior correctly [11, 12].

The aim of this publication is to present different modelling approaches which can be used as approximations for certain situations and which are located between the very simple and the very detailed approaches. Figure 2 illustrates the four new approaches schematically. Different methodologies were used to derive these approaches. Approach A is recommended for BIST collectors with good insulation towards the building interior. The efficiency curve is modified to account for reduced back losses. Approach B is recommended if the heat flux from the absorber to the building is important. A conventional collector model is used and the outputs are modified to account for the thermal coupling between the collector and the building. Approach C can be used, for example, if monitoring data of the solar thermal performance is available. The extended efficiency curve increases the calculation accuracy for the solar thermal performance. Approach D is recommended if measurements of the energy flux to the building interior and of the solar thermal performance e.g. on a test facility are available. The necessary data and effort increase from Approach A to Approach D, as does the accuracy of the models.

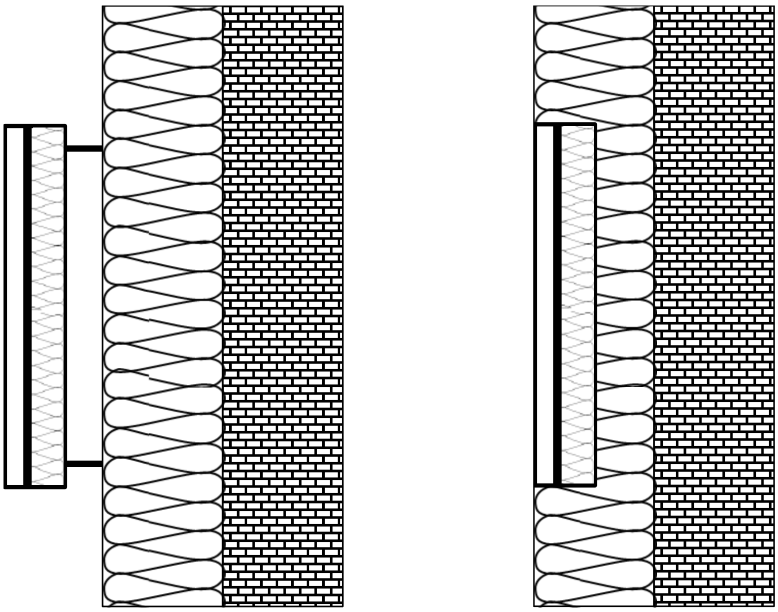

Figure 1 Schematic drawings of a building-added solar thermal collector (BAST, left-hand side) and a building-integrated solar thermal collector (BIST, right-hand side). The solar thermal absorber is indicated by a thick black line, the masonry with a brick pattern and the insulation of the wall and of the collector with insulation batting patterns.

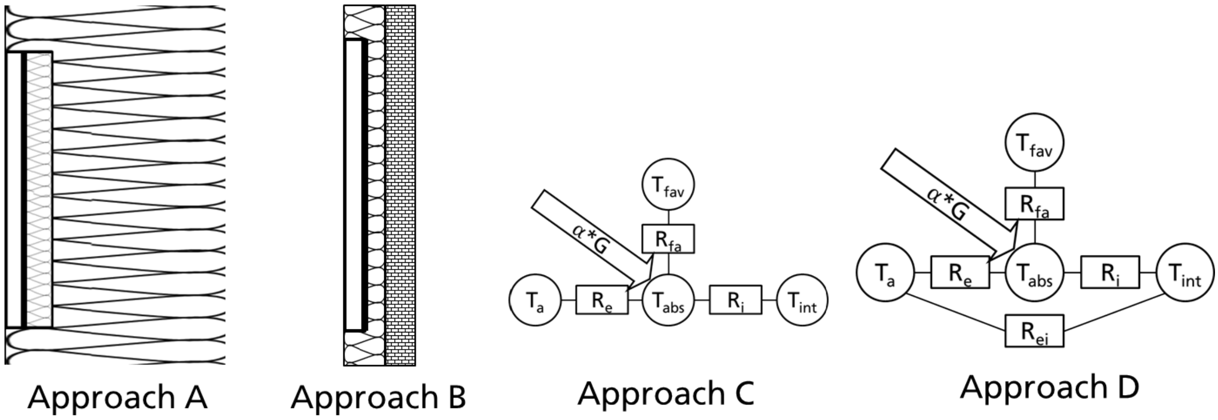

Figure 2 Schematic drawings illustrating the different approaches for modelling building-integrated solar thermal collectors.

3. Theory

3.1. Approach A: Adaptation of the efficiency curve

If the insulation between the absorber of the BIST collector and the building interior is very thick, the heat losses from the absorber to the interior may be neglected. The best solution would be to measure the efficiency curve of this collector with very good insulation of the back and the edges. If this is not possible due to financial or time restrictions and the efficiency curve is known for the BAST case, the following approach can be used to approximate the efficiency curve without back-surface losses. It is based on modifications of the BAST approach of [10].

First, the effective transmittance-absorptance product $(\tau\alpha)_e$ is calculated from the transmittance of the cover glazing τ and the absorptance of the absorber α [13]:

$$(\tau\alpha)_e \cong 1{,}01 * \tau * \alpha \tag{1}$$

With this, the collector efficiency factor F' can be calculated using the efficiency for zero temperature difference between the average fluid temperature and the ambient temperature η_0:

$$\mathrm{F}'_{\mathrm{BAST}} = \frac{\eta_{0,\mathrm{BAST}}}{(\tau\alpha)_{\mathrm{e}}} \tag{2}$$

$(1 - F'_{BAST})$ equals the fraction of thermal losses of already absorbed energy at zero temperature difference between the average fluid temperature and the ambient temperature.

One important parameter is the fraction of thermal losses from the back surface f_{bl} which are avoided by the building integration compared to all thermal losses of a BAST collector. This fraction can be around 1/7 [13].

The fraction of thermal losses through the back of the collector in the BAST case is equal to $(1 - \mathrm{F}'_{\mathrm{BAST}})\mathrm{f}_{\mathrm{bl}}$. The fraction of additional solar thermal gain due to ideal back insulation is equal to $(1 - \mathrm{F}'_{\mathrm{BAST}})\mathrm{f}_{\mathrm{bl}}\mathrm{F}'_{\mathrm{BIST}}$. Without back-surface losses, the collector efficiency factor of the BIST case F'_{BIST} is equal to

$$\mathrm{F}'_{\mathrm{BIST}} = \mathrm{F}'_{\mathrm{BAST}} + (1 - \mathrm{F}'_{\mathrm{BAST}})\mathrm{f}_{\mathrm{bl}}\mathrm{F}'_{\mathrm{BIST}} \tag{3}$$

and therefore

$$\mathrm{F}'_{\mathrm{BIST}} = \mathrm{F}'_{\mathrm{BAST}}/(1 - \mathrm{f}_{\mathrm{bl}} + \mathrm{f}_{\mathrm{bl}}\mathrm{F}'_{\mathrm{BIST}}) \tag{4}$$

The efficiency at zero temperature difference between the average fluid temperature and the ambient temperature in the BIST case $\eta_{0,BIST}$ can be calculated as:

$$\eta_{0,\mathrm{BIST}} = (\tau\alpha)_{\mathrm{e}} * \mathrm{F}'_{\mathrm{BIST}} \tag{5}$$

During stagnation, the mass flow and the efficiency are equal to zero. Therefore $\eta_{0,BAST}$ is equal to:

$$\eta_{0,\mathrm{BAST}} = \mathrm{a}_{1,\mathrm{BAST}}\frac{\Delta \mathrm{T}_{\mathrm{stag,BAST}}}{\mathrm{G}} + \mathrm{a}_{2,\mathrm{BAST}}\frac{(\Delta \mathrm{T}_{\mathrm{stag,BAST}})^2}{\mathrm{G}} \tag{6}$$

The right-hand side of this equation is equal to the thermal losses due to the stagnation temperature. In the BIST case, the fraction f_{bl} of these losses equals the BIST efficiency:

$$\eta_{\mathrm{BIST}}(\Delta \mathrm{T}_{\mathrm{stag,BAST}}) = \eta_{0,\mathrm{BIST}} - \mathrm{a}_{1,\mathrm{BIST}}\frac{\Delta \mathrm{T}_{\mathrm{stag,BAST}}}{\mathrm{G}} - \mathrm{a}_{2,\mathrm{BIST}}\frac{(\Delta \mathrm{T}_{\mathrm{stag,BAST}})^2}{\mathrm{G}} = \mathrm{f}_{\mathrm{bl}}\eta_{0,\mathrm{BAST}}\ . \tag{7}$$

Assuming that

$$\mathrm{a}_{2,\mathrm{BIST}} = \mathrm{a}_{2,\mathrm{BAST}} \tag{8}$$

$a_{1,BIST}$ can be fitted.

In this way, the parameters $\eta_{0,BIST}$, $a_{1,BIST}$ and $a_{2,BIST}$ of the BIST efficiency curve can be calculated from standard BAST parameters. The incidence angle modifier is the same in both cases.

If the thermal coupling between the absorber and the building interior is to be considered, the temperature of the absorber T_{abs} can be approximated by the average fluid temperature $T_{f,av}$. However, a better approximation includes the thermal resistance between the average fluid temperature and the average absorber temperature R_{fa} multiplied by the useful collector gain q_{use}:

$$\mathrm{T}_{\mathrm{abs,op,BIST}} = \mathrm{R}_{\mathrm{fa}}\mathrm{q}_{\mathrm{use,BIST}} + \mathrm{T}_{\mathrm{f,av}} \tag{9}$$

This equation also holds for the BAST case:

$$\mathrm{T}_{\mathrm{abs,op,BAST}} = \mathrm{R}_{\mathrm{fa}}\mathrm{q}_{\mathrm{use,BAST}} + \mathrm{T}_{\mathrm{f,av}} \tag{10}$$

Whenever there is no fluid flow, the stagnation temperature of the absorber T_{stag}

$$T_{abs,stag,BIST} = \Delta T_{stag,BIST} + T_a = \frac{-a_{1,BIST} + \sqrt{a_{1,BIST}^2 + 4a_{2,BIST} G \cdot \eta_{0,BIST}}}{2a_{2,BIST}} + T_a \quad (11)$$

can be used for the absorber temperature T_{abs}.

Within the building model, the façade collector area can be defined to be adiabatic. A more accurate approach is to link the absorber temperature with the building model to include the corresponding heat flux in the building simulation, which was neglected for the calculation of the collector efficiency. Within the TRNSYS simulation environment [14], a simple connection can be realized by estimating the thermal resistance $R_{i,BIST}$ between the absorber and the building interior and calculating the heat transfer into the building q_{int} with the temperatures of the absorber T_{abs} and the interior T_{int}:

$$q_{int} = \frac{T_{abs} - T_{int}}{R_{i,BIST}} \quad (12)$$

If an extremely well insulated wall is used within the building Type, then q_{int} can be inserted directly as additional wall gain. More advanced methods of coupling have been presented by [4, 5].

3.2. Approach B: Adaptation of the collector results

Even if the heat flux between the BIST absorber and the building interior cannot be neglected, the collector may still be simulated as if it were building-attached, using some corrections to approximate the true heat flux to the interior and the increased collector gain.

First, the thermal resistance between the absorber and the interior $R_{i,BIST}$ in the BIST case needs to be calculated as well as the thermal resistance $R_{i,BAST}$ between the absorber and the air behind the back of the of the collector in the BAST case.

As in approach A, the temperature of the absorber T_{abs} can be calculated according to equations (9) and (11).

In each timestep of the simulation, the back losses of the collector can be calculated for the BAST and the BIST case:

$$q_{int,BAST} = \frac{1}{R_{i,BAST}} (T_{abs,BAST} - T_a) \quad (13)$$

$$q_{int,BIST} = \frac{1}{R_{i,BIST}} (T_{abs,BIST} - T_{int}) \quad (14)$$

with the ambient air temprature T_a and the temperature of the building interior T_{int}.

The collector gain $q_{use,BIST}$ of the BIST case can then be approximated by the collector gain $q_{use,BAST}$ and the back losses $q_{int,BAST}$ and $q_{int,BIST}$ of the two different cases:

$$q_{use,BIST} = q_{use,BAST} + q_{int,BAST} - q_{int,BIST} \tag{15}$$

Combining the equations (9), (10) (13), (14) and (15) for cases with fluid flow leads to

$$q_{use,BIST} = (q_{use,BAST} R_{i,BIST}\left(R_{fa} + R_{i,BAST}\right) + R_{i,BIST}(T_{fav} - T_a) + R_{i,BAST}(T_{int} - T_{fav})) \\ /(R_{i,BAST}\left(R_{fa} + R_{i,BIST}\right)) \tag{16}$$

As in approach A, the absorber temperature needs to be calculated by equation (11) whenever there is no fluid flow and needs to be linked to the building model to include the heat flux of the BIST area in the building simulation.

3.3. Approach C: Extended efficiency curve

An extended efficiency curve including the temperature of the building interior was proposed by [12].

There the efficiency η depends on the temperature of the ambient as well as of the building interior:

$$\eta = \eta_0 - a_{1,ext} * x - a_{2,ext} * x^2 * G - a_{1,int} * y - a_{2,int} * y^2 * G \tag{17}$$

with

- $x = \frac{T_{fav} - T_a}{G}$ [m^2*K *W^{-1}]
- $y = \frac{T_{fav} - T_{int}}{G}$ [m^2*K* W^{-1}]
- $a_{1,int}$: internal linear heat loss coefficient [W*K^{-1}*m^{-2}]
- $a_{2,int}$: internal second-order heat loss coefficient [W* K^{-2*} m^{-2}]
- $a_{1,ext}$: external linear heat loss coefficient [W*K^{-1}*m^{-2}]
- $a_{2,ext}$: external second-order heat loss coefficient [W*K^{-2}*m^{-2}]
- G: total irradiance on the collector surface [W*m^{-2}]
- $T_{fav} = \frac{a_{1,int} + T_{fo}}{2}$: the mean fluid temperature in the collector
- T_{int}: the temperature of the building interior
- T_a: the ambient temperature
- η_0: the efficiency at zero temperature difference between the fluid, the front and the back of the collector.

The assumption is that equation (17) better describes a BIST collector than the standard efficiency curve

$$\eta = \eta_0 - a_1 * x - a_2 * x^2 * G \tag{18}$$

from [10], because it includes the losses to the building interior q_{int} by

$$q_{int} = a_{1,int} * y * G + a_{2,int} * y^2 * G^2. \tag{19}$$

However, this is only true for the collector gain. The uncertainty of this approach for the heat flux to the building interior was high, e.g. equal to 48 W/m^2 in comparison to a detailed physical collector model [12].

If the thermal resistance between the absorber and the building interior is known and if the parameters $\eta_0, a_{1,ext}, a_{2,ext}, a_{1,int}$ and $a_{2,int}$ fit well to the real collector gain, then the temperature of the absorber during operation can be calculated by equation (9). For cases without fluid flow, the absorber temperature can be calculated by

$$\mathrm{T_{abs,stag}} = \frac{1}{2(\mathrm{a_{2,ext}}+\mathrm{a_{2,int}})}\Big(-\mathrm{a_{1,ext}} - \mathrm{a_{1,int}} + 2\mathrm{a_{2,ext}}\mathrm{T_a} + 2\mathrm{a_{2,int}}\mathrm{T_{int}} + \Big(\big(-\mathrm{a_{1,ext}} - \mathrm{a_{1,int}} + 2\mathrm{a_{2,ext}}\mathrm{T_a} + 2\mathrm{a_{2,int}}\mathrm{T_{int}}\big)^2 + 4\big(\mathrm{a_{2,ext}} + \mathrm{a_{2,int}}\big)\big(\eta_0 \mathrm{G} + \mathrm{a_{1,ext}}\mathrm{T_a} - \mathrm{a_{2,ext}}\mathrm{T_a^2} + \mathrm{a_{1,int}}\mathrm{T_{int}} - \mathrm{a_{2,int}}\mathrm{T_{int}^2}\big)\Big)^{0.5}\Big) \tag{20}$$

The heat flux to the interior is then better calculated by

$$\mathrm{q_{int}} = \frac{1}{\mathrm{R_{i,BIST}}}(\mathrm{T_{abs}} - \mathrm{T_{int}}) \tag{21}$$

than by equation (19).

3.4. Approach D: Simple node model

As an example of simple node models, the model presented in Figure 2 is investigated. The parallel resistance R_{ei} of this model can account for heat flux around the collector edges.

To assess this approach, the detailed physical model of [11] was used to calculate 2520 different cases. The following values were combined with each other: ambient temperatures of -20, 0, 20 and 40 °C, indoor temperatures of 0, 10, 20, 30 and 40 °C, fluid mass flow rates of 0 and 0.02 kg/(m^{2}s), fluid inlet temperatures of 5, 15, 25, 35, 45, 55, 65, 75 and 85 °C and irradiance values of 0, 200, 400, 600, 800, 1000 and 1200 W/m^2. The cases cover most situations in a Central European climate, but are not representative in their distribution.

The thermal resistances R_e, R_i, R_{ei}, R_{fa} and the absorptance α were then varied to minimize the differences between the detailed physical model and the simple node model.

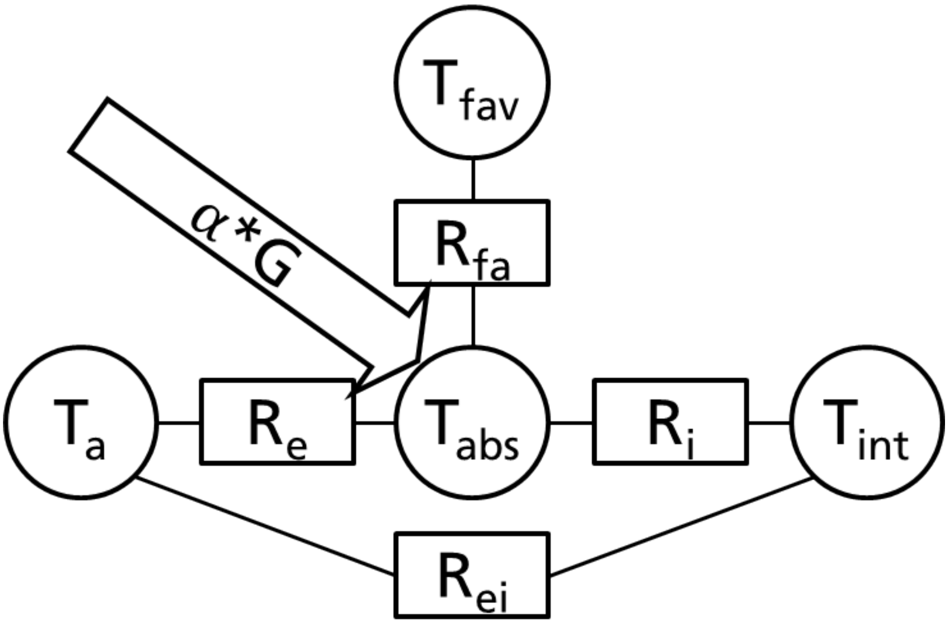

Figure 3 Schematic drawing of the simple node model. There is a parallel thermal resistance R_{ei} between the temperatures of the ambient air $T_a$and the building interior T_{int}. The absorber temperature T_{abs} is connected to T_a by the thermal resistance R_e and to T_{int} by the thermal resistance R_i. The absorber receives the absorbed radiation αG and is connected by the thermal resistance R_{fa} to the average fluid temperature T_{fav}.

4. Results and Discussion

If no simple model is used and the coupling between the absorber and the building interior is neglected, then the heat flux from the building interior to the BIST element is overestimated in winter and the heat flux from the BIST element to the building interior is underestimated in summer. Also, the collector gain is underestimated throughout the whole year.

If we assume a U value of 0.15 W/(m^{2}K) and a winter day with an ambient temperature of 0 °C and a room temperature of 20 °C then a calculation with a zero g value for the façade leads to heat losses of 3.1 W/m^2. If we assume a surface temperature of the conventional façade of 3.5 °C and a BIST absorber temperature of 25 °C, then heat losses of 2.5 W/m^2 result for the conventional façade while at the BIST areas, a heat gain of 0.8 W/m^2 occurs. Without coupling, the heat losses from the BIST area are therefore overestimated by more than 3 W/m^2 in this situation.

If we assume a summer day with an ambient temperature of 30 °C, a room temperature of 25 °C, a surface temperature of the conventional façade of 45 °C and a BIST absorber temperature of 65 °C, then a pure U value calculation leads to heat gains of 0.8 W/m^2. If the temperature of the façade surface is considered, a heat flux of 3.1 W/m^2 is calculated and for the BIST areas, the heat flux amounts to 6.2 W/m^2. Without coupling, the heat gains through the BIST area are therefore underestimated by 3.1 W/m^2 in this situation.

4.1. Approach A: Adaptation of the efficiency curve

Figure 3 presents the efficiency curves for a BAST collector[1] together with the derived efficiency curves for the BIST case (f_{bl}=1/7) as well as for a BIST_0.9bl case with the fraction of back losses reduced by 10%. The relative error between the BIST calculation and a simulation without coupling (BAST) increases with increasing temperature difference between the fluid T_{fav} and the ambient T_a and decreasing irradiance G. At the BIST stagnation temperature, the absolute error of the efficiency amounts to 0.12 which equals 120 W/m^2 at an irradiance of 1000 W/m^2.

If the fraction of back losses is overestimated by 10%, an absolute error of 0.012 results at the BIST stagnation temperature. A certain degree of uncertainty in calculating the fraction of back losses can therefore be tolerated.

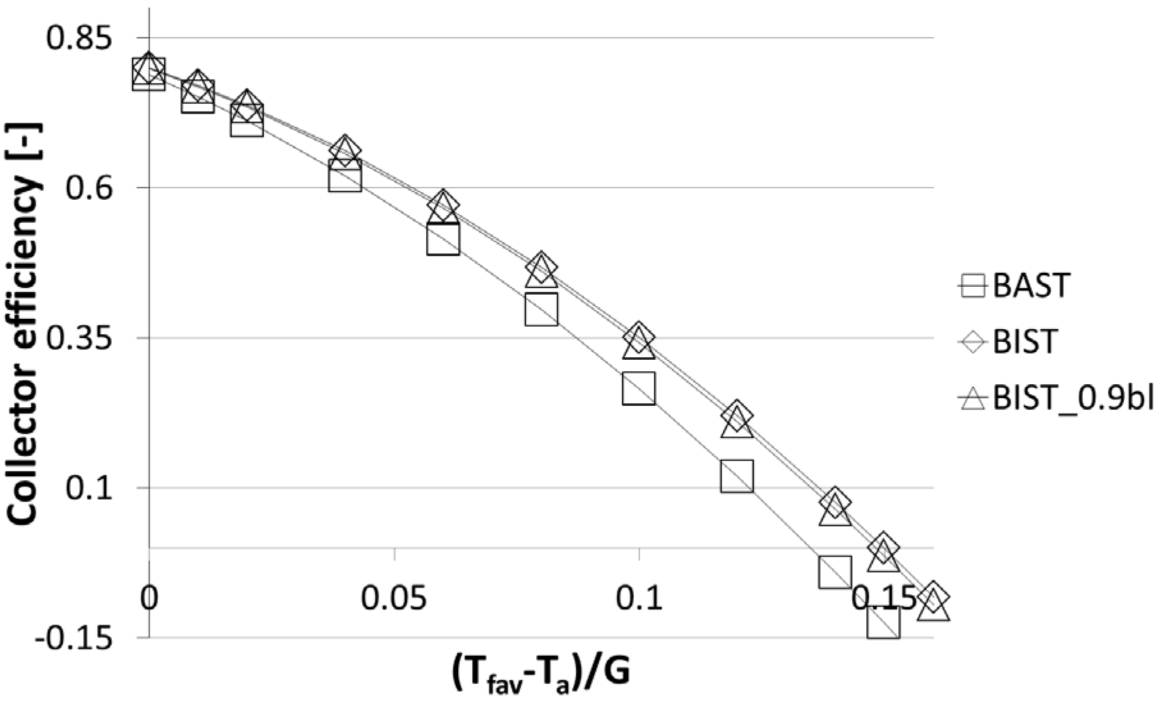

Figure 4 Efficiency of the collectors depending on the temperature difference between the fluid T_{fav} and the ambient T_a and the irradiance G for the BAST case, the BIST case and the BIST_0.9bl case with a smaller fraction of back losses.

---

[1] $\eta_{0,BIST}$ = 0.789; $a_{1,BIST}$= 3.545; $a_{2,BIST}$ = 0.017; τ = 0.91; α = 0.95.

If the useful collector gain calculated by the BIST efficiency curve is used to calculate the absorber temperature according to equation (9), the heat flux to the building should be quite accurate, depending only on the uncertainties of the efficiency curve and of the thermal resistance between the absorber and the fluid R_{fa}. The thermal capacity of the BIST is not integrated into approach A, but can be implemented in the façade description of the building model.

The largest error of Approach A is that it assumes a constant fraction of back losses. The efficiency and the absorber temperature depend only on the ambient temperature and not on the temperature of the building interior. This error increases with decreasing thermal resistance between the absorber and the building interior and with increasing temperature difference between the temperatures of the ambient and of the building interior. Therefore, Approach A can be recommended especially for high insulation values between the absorber and the building interior.

If we take the BIST collector of Figure 3 and assume an ambient temperature of 0 °C, a temperature of the building interior of 20 °C, an irradiance of 100 W/m^2 on the façade, stagnation conditions and a U value of 0.24 W/(m^{2}K), Approach A leads to an absorber temperature of 24.9 °C. If we assume that all thermal losses of the collector flow to the ambient, a thermal resistance between the absorber and the ambient of 0.31 (m^{2}K)/W results. If this is used for an energy balance including the heat flux to the building interior, an absorber temperature of 26.5 °C is calculated. The heat flux into the building is therefore underestimated by 0.5 W/m^2 in this case by neglecting the temperature of the interior in the calculation of the collector gain.

The accuracy could be further improved by using a weighted average between the temperatures of the ambient and of the interior to calculate the collector gain. However, the collector losses are not linear which leads to a complexity similar to the nodal model presented in approach D.

4.2. Approach B: Adaptation of the collector results

In Approach B, the temperature of the building interior is included in the calculation of the collector gain and therefore also in the calculation of the absorber temperature.

If we assume a U value of 0.24 W/(m^{2}K), an ambient temperature of 30 °C, a temperature of the building interior of 25 °C, an irradiance of 1000 W/m^2 on the façade and back losses of 1/7, the absorber reaches a stagnation temperature of 165°C in the BAST case. In the BIST case, the stagnation temperature is 180°C according to the parameters from approach A. If the BAST parameters are used instead of deriving BIST parameters for equation (11), then the heat flux to the building interior would be underestimated by 4 W/m^2. If we assume operating conditions with a thermal resistance between the absorber and the fluid of 0.0165 (m^2K)/W, a thermal resistance between the absorber and the air behind the absorber $R_{i,BAST}$ of 0.81 (m^2K)/W and between the absorber and the interior $R_{i,BIST}$ of 0.27 (m^2K)/W, and a BAST collector gain $q_{use,BAST}$ of 667 W/m^2, then a BIST collector gain $q_{use,BIST}$ of 705 W/m^2 results, as compared to 701 W/m^2 with approach A. If $R_{i,BAST}$ is decreased by 10% and $R_{i,BIST}$ is increased by 10%, a BIST collector gain of 713 W/m^2 results. The absorber temperature varies by only 0.14 °C. Small errors in the calculation of $R_{i,BAST}$ and $R_{i,BIST}$ therefore seem to be tolerable in typical cases.

4.3. Approach C: Extended efficiency curve

The accuracy of approach C depends on the accuracy of the parameters η_0, $a_{1,ext}$, $a_{2,ext}$, $a_{1,int}$ and $a_{2,int}$ and the thermal resistance between the absorber and the interior $R_{i,BIST}$. As presented in [12], the extended efficiency curve achieves a root-mean-square error (RMSE) of 0.0023 for the efficiency compared to 0.0112 for the standard efficiency curve. This means that the benefit of the extended efficiency curve is limited. However, if e.g. monitoring data is available to fit the efficiency curve, the extended efficiency curve should be used because it provides higher accuracy at little extra effort. If only the BAST efficiency curve is known, Approach B is recommended. If $R_{i,BIST}$is overestimated by 10%, then q_{int} is underestimated by 9%. $R_{i,BIST}$ should therefore be calculated carefully.

4.4. Approach D: Simple node model

The comparison between the simple node model of approach D and the detailed physical model lead to a root mean square error (RMSE) of 2 W/m^2 for the heat flux to the building interior and of 13 W/m^2 for the collector gain. At an average absolute value of 28 W/m^2 for the heat flux to the interior and of 152 W/m^2 for the collector gain when the collector is operating, the uncertainty of the heat flux to the interior and of the collector gain can be estimated to be 8%. Other parameter sets can reduce the RMSE for one heat flux while increasing the RMSE for the other heat flux.

If instead of Approach D, the standard BAST approach is used and the standard efficiency curve is fitted to results of the detailed model, then the thermal coupling is neglected and a RMSE of the collector gain of 240 W/m^2 results. Therefore the BAST approach should not be used when there is significant thermal coupling between the collector and the building.

By limiting the cases to realistic and typical situations, the accuracy can be further improved with the risk of large errors in rare cases.By including more parameters, the accuracy of the model can be improved as well. There is a large variety of possible node models between this simple model and a detailed physical model.

4.5. Comparison of the approaches

From Approach A to Approach D, the required quality of the necessary input increases. Approach A only needs the efficiency parameters of the collector datasheet. It is well suited for good insulation between the absorber and the building interior. When the heat flux between the absorber and the interior becomes relevant, Approach B is recommended. It needs a little more effort than Approach A, but still delivers accurate results without additional measurements. If measurement results are available, for instance from a demonstration installation, the efficiency curve (17) can be fitted to this data and provides a more accurate calculation of collector gain, stagnation temperature and heat flux to the interior than Approaches A and B, since it includes the influence of real integration including e.g. edge effects. For new BIST elements, simultaneaous measurements of the collector gain and the heat flux to the interior are recommended to calibrate the simple model of Approach D. This already allows an analysis of the benefits of the new component under various conditions. If high accuracy in certain situations is needed, the model of Approach D can be easily extended to include additional relevant physical effects. If the the absorber temperature is set to the ambient temperature in the night case (no irradiance, no fluid flow), then the heat loss of the building does not include the thermal resistance between the ambient and the absorber. If the building is well insulated, this may have negligible effect. For less-well insulated buildings or higher accuracy, the U value of the BIST building envelope can be used instead of R_i in this case.

5. Conclusion

This paper presented four new and simple models for BIST façade elements. With these models, the thermal coupling of BIST collectors and the building can be taken into account. Depending on the available data, an approach with acceptable uncertainty can be chosen. Approach A is recommended for buildings with good insulation between the absorber and the building interior. Approach B is recommended for cases when the heat flux between the absorber and the building interior cannot be neglected. If monitoring data of the BIST solar thermal performance are available, Approach C can be useful with its improved formula for the collector efficiency. If measurements of the energy flux to the interior and of the solar thermal performance, e.g. on a BIST test facility are available, the model of Approach D can be calibrated and characterizes the BIST building envelope well. The necessary data and effort increase from Approach A to Approach D, as does the accuracy of the models. Based on this analysis, further models can be developed to reduce the remaining uncertainties. For instance, a correction could be developed to derive the efficiency curve of vertically installed collectors from the parameters extracted from measurements on tilted collectors. In the future, a standard for models of active façade elements will be helpful to ensure the quality of a model provided to the planner.

6. Acknowledgement

This work was funded by the German Federal Ministry for Economic Affairs and Energy, based on a decision by the German Bundestag. The authors thank the European Union for support in COST Action TU1205- BISTS, Michael Hermann for valuable discussions and Helen Rose Wilson for proofreading this paper.

7. Nomenclature

SYMBOL	EXPLANATION
α	Absorptance of the absorber in the collector
$a_1, a_{1,BAST}, a_{1,BIST}, a_{1,ext}, a_{1,int}$	First-order collector efficiency coefficients in general, in the BAST case, in the BIST case, for the exterior, for the interior (W/(m^{2}K))
$a_2, a_{2,BAST}, a_{2,BIST}, a_{2,ext}, a_{2,int}$	Second-order collector efficiency coefficients in general, in the BAST case, in the BIST case, for the exterior, for the interior (W/(m^{2}K^2))
BAST	Building-added solar thermal
BIST	Building-integrated solar thermal
F'	Collector efficiency factor
G	Solar irradiance (W/m^2)
$\eta, \eta_{BAST}, \eta_{BIST}, \eta_0, \eta_{0,BAST}, \eta_{0,BIST},$	Collector efficiency η=η_0-a_1x-a_2x^2G in general, in the BAST case, in the BIST case, collector efficiency at x=0, in the BAST case, in the BIST case,
$q_{use}, q_{use,BAST}, q_{use,BIST}$	Solar thermal collector gain in general, in the BAST case and in the BIST case (W/m^2)
q_{int}	Heat transfer from the collector to the building interior (W/m^2)
$R_e, R_{e,BAST}, R_{e,BIST}$	Thermal resistance between the absorber and the ambient temperature in general, for the BAST case, for the BIST case (m^{2}K/W)
R_{fa}	Thermal resistance between the absorber and the average fluid temperature (m^{2}K/W)
$R_i, R_{i,BAST}, R_{i,BIST}$	Thermal resistance between the absorber and the temperature of the

	building interior in general, for the BAST case, for the BIST case (m^2K/W)
RMSE	Root-mean-square error
τ	Transmittance of the cover of the collector
$(\tau\alpha)_e$	Effective transmittance-absorptance product
TSTC	Transparent solar thermal collector
T_a , T_{int} , T_{fav} , T_{fi} , T_{fo} , T_{abs} , $T_{abs,op}$, $T_{abs,sta}$	Temperature of the ambient air, of the building interior, of the fluid (average), of the fluid inlet, of the fluid outlet, of the absorber, of the absorber during collector operation and of the absorber during stagnation (K)
U	U value ($W/(m^2K)$)
x	Difference between the average fluid temperature and the ambient temperature divided by the solar irradiance (m^2K/W)
y	Difference between the average fluid temperature and the temperature of the building interior divided by the solar irradiance (m^2K/W)

8. References

[1] C. Plantier, G. Fraisse, G. Achard, Development and experimental validation of a detailed flat-plate solar collector model, ISES Solar World Congress, International Solar Energy Society (ISES), Göteborg, Sweden, 14-19 June 2003.

[2] M.A. Hassan, Y. Beliveau, Design, construction and performance prediction of integrated solar roof collectors using finite element analysis, Construction and Building Materials, 21 (5) (2007) 1069-1078, doi:DOI 10.1016/j.conbuildmat.2006.01.

[3] J. Cadafalch, A detailed numerical model for flat-plate solar thermal devices, Solar Energy, 83 (12) (2009) 2157-2164, doi:DOI 10.1016/j.solener.2009.08.013.

[4] C. Maurer, T.E. Kuhn, Variable g value of transparent façade collectors, Energy and Buildings, 51 (2012) 177-184, doi:10.1016/j.enbuild.2012.05.011.

[5] M. Hauer, A. Richtfeld, W. Streicher, P. Hauser, Gekoppeltes TRNSYS-Modell zur thermischen Bewertung von Fassadenkollektoren, e-nova-Konferenz, Pinkafeld, 22.-23. December 2012.

[6] M. Hauer, A. Richtfeld, W. Streicher, Gebäudegekoppelte Simulation fassadenintegrierter Kollektoren mit TRNSYS, 23. OTTI-Solarthermie Symposium, Bad Staffelstein, 24-26 April 2013.

[7] C. Lamnatou, J.D. Mondol, D. Chemisana, C. Maurer, Modelling and simulation of Building-Integrated solar thermal systems: Behaviour of the coupled building/system configuration, Renewable and Sustainable Energy Reviews, 48 (0) (2015) 178-191, doi:http://dx.doi.org/10.1016/j.rser.2015.03.075.

[8] C. Lamnatou, J.D. Mondol, D. Chemisana, C. Maurer, Modelling and simulation of Building-Integrated solar thermal systems: Behaviour of the system, Renewable and Sustainable Energy Reviews, 45 (0) (2015) 36-51, doi:http://dx.doi.org/10.1016/j.rser.2015.01.024.

[9] C. Maurer, Theoretical and experimental analysis and optimization of semi-transparent solar thermal façade collectors, Dissertation, Fakultät für Architektur, Karlsruher Institut für Technologie (KIT), 2012, doi:10.13140/2.1.3979.9686.

[10] P.I. Cooper, R.V. Dunkle, A non-linear flat-plate collector model, Solar Energy, 26 (2) (1980) 133-140, doi:10.1016/0038-092X(81)90076-1.

[11] C. Maurer, T. Baumann, M. Hermann, P. Di Lauro, S. Pavan, L. Michel, T.E. Kuhn, Heating and cooling in high-rise buildings using facade-integrated transparent solar thermal collector systems, Journal of Building Performance Simulation, 6 (6) (2013) 449-457, doi:10.1080/19401493.2013.766263.

[12] T. Pflug, P. Di Lauro, T.E. Kuhn, C. Maurer, Evaluation of a simplified model for façade collectors, Building Simulation Conference, IBPSA, Chambéry, France, 25-28 August 2013, doi:10.13140/2.1.4569.7925.

[13] J.A. Duffie, W.A. Beckman, Solar engineering of thermal processes, 3rd ed., Wiley, Hoboken N.J., 2006.

[14] W.A. Beckman, L. Broman, A. Fiksel, S.A. Klein, E. Lindberg, M. Schuler, J. Thornton, TRNSYS The most complete solar energy system modelling and simulation software, Renewable Energy, 5 (1-4) (1994) 486-488, doi:10.1016/0960-1481(94)90420-0.